Free-Jet Expansions from Laser-Vaporized Planar Surfaces

M. Alan Covington,* George N. Liu,† and Kenneth A. Lincoln‡
NASA Ames Research Center, Moffett Field, Calif.

Characteristics of free-jet vapor expansions created by the pulsed-laser vaporization of some carbon materials are examined. Such expansions were generated from planar surfaces at laser power densities up to 2.5 MW/cm^2. Time-integrated and time-resolved photography was used to show that the structure and pressures of such flows are correlated by the same relationship that is valid for free jets from orifice flows. Data show that the vapor velocity becomes sonic at or very near the vaporizing surface. A method is presented for deriving vaporization pressure from flowfield photos, and such pressures from carbon vaporization for temperatures to 4500 K are in good agreement with extrapolated equilibrium vapor pressures. It is shown that this technique may be a new way to determine vapor pressures of refractory materials at high temperatures.

Introduction

THE behavior of vapor clouds resulting from the vaporization of solid matter by high-power, pulsed lasers has been extensively studied, but not all of the associated phenomena are well understood. Past work using Q-switched and normal mode lasers[1,2] has considered both phase change and the thermodynamic state at the vaporizing surface and the gasdynamic motion of the induced vapor clouds. For vaporization using Q-switched lasers with pulse lengths of 10^{-9}-10^{-7} sec, energy deposition occurs in times much shorter than those required for the gasdynamic flow of vaporized material away from the surface (10^{-6}-10^{-5} sec), and the situation approaches that of the sudden expansion of an initially spherical vapor cloud into vacuum.[3] This is in contrast to vaporization using normal, or burst, mode pulsed lasers where the typical heating times of 10^{-5}-10^{-3} sec are comparable to or much longer than the characteristic gasdynamic flow times.[2,4] For the latter situation, the vaporization and vapor expansion processes can be considered quasisteady.

The phenomenon considered here is the quasisteady, supersonic, free-jet expansion of vapor products from the high-power, pulsed-laser vaporization of solids. Earlier works[4,5] have predicted or observed such free jets, but the conditions under which they occur and their characteristics have not been investigated extensively. Data are presented that show some characteristics of these "vaporization free jets," and a comparison is made with free-jet expansions from orifice sources. These data were obtained under experimental conditions in which absorption of laser energy by vaporized and ambient gas species was negligible and with the pressure at the vaporizing surface greater than the ambient pressure. The results given are from the vaporization of three forms of carbon (ATJ and pyrolytic graphites, vitreous) although similar flows also have been observed during the laser heating of alumina, silicon carbide, and the nitrides of aluminum, boron, and silicon.

Experimental Apparatus and Technique

All vaporization experiments were conducted in a vacuum chamber formed as a right circular cylinder (Fig. 1) with an inside diameter of 34.5 cm and a length of 17.5 cm. The cylinder was closed at one end and the other end was fitted with a window of either glass or lucite to allow viewing of the entire inside volume of the chamber. Ports around the periphery of the chamber permitted installation of a material sample holder and several small windows used for entrance of the indicent laser beam and for viewing the vaporizing surface with a pyrometer. A mechanical vacuum pump allowed the pressure within the sealed chamber to be held constant at levels between 1 atm and a few microns.

Material samples positioned within this vacuum chamber were irradiated by the focused beam from a neodymium-glass (1.06-μm wavelength) laser operated in the normal, or burst, mode with pulse durations up to 1 msec. The range of laser operating conditions used is given in Table 1. A beam-splitter directed a fraction of the laser beam energy into a radiometer, which measured the pulse shape and total energy of each laser pulse. The sample holder within the chamber permitted the incident angle between the laser beam and the sample surface to be varied from 0 to 90 deg.

A limited amount of surface temperature data was obtained using a silicon photodetector pyrometer in conjunction with optical interference filters. These filters minimized problems of reflected laser beam radiation and of emission spectra from the hot vapor species themselves and allowed sensing of only the radiation coming from the heated solid surface. The small focal spot (0.50 mm^2) and relatively short time constant ($\sim$10 μsec) of this pyrometer made it possible to measure the temperature of small regions within the larger irradiated area as a function of time. These time-resolved surface temperatures were correlated with derived vaporization pressure, as will be presented later.

Photographic data on the free jets from laser-vaporized surfaces were obtained by two techniques. In one method, a conventional camera was used to obtain time-integrated images of the luminous jet structure. In the other method, a high-speed, electro-optical framing camera was used to obtain

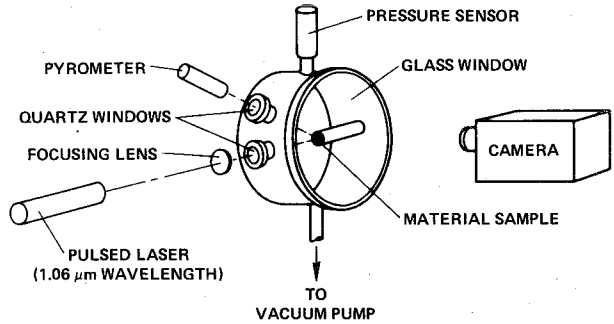

Fig. 1 Experimental arrangement.

Presented as Paper 76-22 at the AIAA 14th Aerospace Sciences Meeting, Washington, D.C., Jan. 26-28, 1976; submitted March 11, 1976; revision received May 10, 1977.

Index categories: Jets, Wakes, and Viscid-Inviscid Flow Interactions; Lasers; Thermochemistry and Chemical Kinetics.

*Research Scientist. Member AIAA.

†NRC Research Associate; presently Research Associate, Stanford University. Member AIAA.

‡Research Scientist.

Table 1 Laser heating conditions

Wavelength	1.06 μm
Operating mode	Normal (burst)
Pulse duration	Approx. 1/3-1 msec
Energy density on target	50-1200 J/cm^2
Peak irradiance	200-2500 kW/cm^2
Beam diameter on target	Approx. 2-5 mm

sequential images of the free jet as it progressed from its initial formation, through maximum development, to its decay at the end of the laser heating pulse. This high-speed camera, employing a triggered image-converter tube, allowed images to be formed with varying time intervals between frames and with varying exposure time per frame. Different periods of the free-jet lifetime were covered by varying the delay time between the starting of the laser pulse and the triggering of the framing camera.

Experimental data on the angular distribution of mass flux within the expanding flow were measured by a deposition technique. After vaporization of a sample positioned at the center of the test chamber, the relative thickness of the condensed film along and across a thin plastic sheet fitted around the chamber inside periphery was measured with an optical densitometer to determine the integrated mass flow distribution.

Spatial and temporal beam nonuniformities typical of solid-state lasers operated in the burst mode were found to have negligible effects. The particular laser used exhibited a fairly uniform flux distribution, and some indirect beam uniformity measurements and effects on jet structure are discussed later. It has been observed that burst-mode laser radiation is typically composed of a series of microsecond-duration spiked pulses rather than a continuous emission,[2] but surface temperature oscillations due to these spiked pulses are damped by thermal capacitance and vaporization mechanisms.[4] Since the resulting variations in material vaporization rate occur on a smaller time scale (10^{-6} sec) than the characteristic time for vapor flow, it is expected that the gasdynamic expansion uncouples the effects of the microsecond heating spikes on free-jet structure away from the vaporizing surface.

Results and Discussion

Free-Jet Characteristics

A typical time-integrated photo of a free jet generated by surface vaporization of ATJ graphite is shown in Fig. 2. The background gas was air at a constant pressure of 23 Torr, and the area heated by the focused laser beam was 4.9 mm^2. The features of an underexpanded, supersonic free jet are easily identified: the barrel shock with an associated outer mixing layer, and the characteristic planar, standing shock wave, or Mach disk, some distance x downstream of the source. It should be noted that the laser-induced vaporization taking place within the bright area of diameter D seen in Fig. 2 is occurring on a clean, planar surface without a significant crater or hole with only about 50 μm of material removed for each laser pulse. Similar free-jet expansions have been observed on planar graphite surfaces at lower heating rates with lesser mass removal (5-10 μm) and from a uniformly ablating graphite rod end being fully irradiated by a laser beam.

Figure 3 shows that conditions within the flow between the vaporizing surface and the Mach disk are supersonic. In this time-integrated photograph, a detached shock wave in front of a thin rod held across the jet is clearly shown. The portion of the Mach disk remaining in the lower part of the flow undisturbed by the rod shock as well as the radial nature of the flow coming from the surface are both apparent.

Vaporizations of graphite were carried out in an inert ambient gas as well as in air to see if reactions between oxygen and nitrogen and vaporized species in the expanding flows contributed to the observed luminosity or structure of the free jets. Figure 4, which shows a free jet from the vaporization of ATJ graphite expanding into argon, indicates that such reactions are not important in the flow upstream of the Mach disk. It would be expected that these reactions are important only if the ambient gases can diffuse into the vapor flowfield faster than they are carried downstream in the bulk flow. A comparison of characteristic times for diffusion and flow shows that diffusional effects are unimportant in the free jets considered here. We may define these times as $\tau_d = \delta^2/\mathfrak{D}$ and $\tau_f = \delta/\bar{u}$ where τ_d and τ_f are the times for diffusion and flow, respectively, δ is a typical dimension of the jet, $\mathfrak{D}$ is the diffusion coefficient for the ambient gas migrating into the vapor, and $\bar{u}$ is the flow velocity. Between the vaporizing surface and the Mach disk $\delta \approx 1$ cm, $\bar{u} > 10^5$ cm/sec, and $\mathfrak{D} < 100$ cm^2/sec for the conditions investigated. It can be seen that diffusion effects can be neglected since $\tau_d \gg \tau_f$. It can be concluded that the observed photographic images of the barrel shock and Mach disk are caused by emission from excited atomic and molecular vapor species in the flow and not by any reactions with ambient gases.

Gas-phase interaction of vaporized material with the incident laser radiation depends on the chemical species present and their vapor density as well as both the laser beam

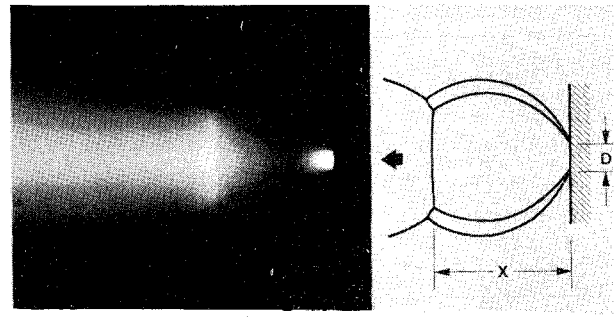

Fig. 2 Free-jet expansion of vapors from laser-heated graphite in air: pulse length ≈ 800 μsec; wavelength = 1.06 μm; $q_{max} = 9.1 \times 10^5$ W/cm^2; $P_f = 23$ Torr.

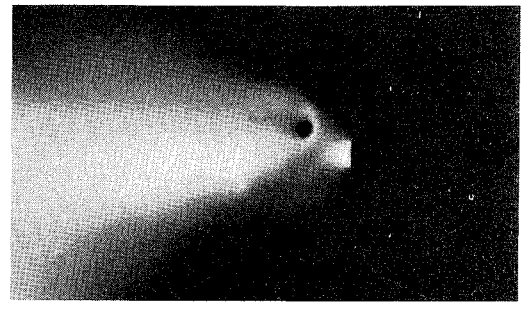

Fig. 3 Standing shock from transverse rod within jet from laser-heated graphite: $P_f = 25$ Torr; $E \cong 300$ J/cm^2; rod diam = 1.6 mm.

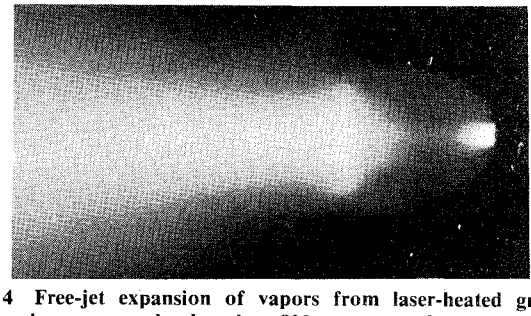

Fig. 4 Free-jet expansion of vapors from laser-heated graphite surface in argon: pulse length $\simeq 800$ μsec; wavelength = 1.06 μm; $q_{max} = 9.2 \times 10^5$ W/cm^2; $P_f = 25$ Torr.

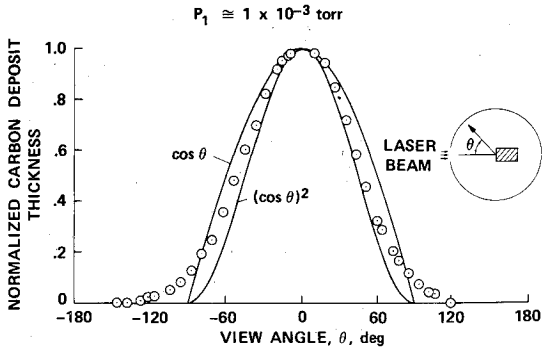

Fig. 5 Angular distribution of mass flux in plumes from laser vaporized graphite.

wavelength and intensity. Experiments in which carbon samples were irradiated at varying beam incident angle have shown that such interaction effects are unimportant over the range of conditions given in Table 1. The vapor flow was normal to the planar surface for incident angles up to 45 deg, and there was no distortion of the free-jet structure that might be evident if significant gas-phase absorption of laser energy occurred.

The angular distribution of mass flux within free-jet expansions into vacuum from graphite was measured as previously described. The results given in Fig. 5 for points within a plane through and normal to the vaporized surface area, and equidistant from the center of the area, suggest that the mass flux is approximated by a $\cos^n\theta$ $(1 \leq n \leq 2)$ distribution, where θ is the angle between a given streamline and a line normal to the surface. Although not investigated, the "tails" of the distribution at angles greater than 60 deg from the normal are thought to be due to collisional effects near the wall since the data were taken at a pressure where the mean free path in the expanded vapor was smaller than the chamber dimensions. It has been found[6] that highly underexpanded, steady free jets from sonic orifices exhibit a simple, self-similar, isentropic flow with the streamlines appearing to radiate from a point source. For such flows, the density field at a constant radius some distance away from the source was found to obey a $\cos^2\theta$ relationship. Since the flow velocity, u, in a jet expanding into vacuum reaches some maximum value within a short distance from the source and remains essentially constant during subsequent expansion, the mass flux, ρu, angular variation is also described by the same $\cos^2\theta$ distribution. It is evident from Fig. 5 that the mass flow variation across free jets from sonic orifices and these vaporization sources are essentially the same.

In addition to the time-integrated photographic data presented above, time-resolved, high-speed photography was also used to record the development and decay of vaporization free jets. As previously described, an electro-optical framing camera was used to obtain sequential photos of free-jet time histories as shown in Fig. 6. The images shown are from the pulsed vaporization of ATJ graphite under conditions identical to those of the time-integrated photo of Fig. 2. This series of photos is a composite from three separate laser heating pulses under the same conditions. Once the vaporization starts the free-jet structure is seen to form and exist until the surface and vapor temperatures drop to a level where the gaseous species are no longer self-luminous and the vaporization rates become small. An interesting feature in these photos is the series of oblique waves, or Mach diamonds, that can be seen at 670 μsec.

It is seen in Fig. 6 that the Mach disk location and size varies during the laser pulse. The disk initially moves away from the vaporizing surface, reaches a maximum displacement and diameter, and then moves back toward the surface as would be expected for a sonic free jet from a reservoir with varying total pressure. The motion and diameter variation of the planar shock wave during development and decay thus can create the center streak and cone images in time-integrated photographs, such as Figs. 2 and 4. The Mach disk image in such photos is brightest at its maximum distance from the surface since this position corresponds to the highest temperature and density conditions when the hot vapors radiate most strongly. Simultaneous surface temperature measurements have shown that the maximum displacement of the standing shock from the vaporizing surface occurs at the same time as peak surface temperature and pressure. The flow expansion therefore can be considered quasisteady with the Mach disk location related to surface vaporization conditions without time lag.

The characteristics of free jets from steady sonic orifice sources have been extensively investigated. It has been found[6] that the Mach disk location can be correlated by the empirical relation

$$x/D = 0.67(P_0/P_1)^{1/2} \tag{1}$$

where x is the axial distance between the Mach disk and the orifice, D is the orifice diameter, P_0 is the total (reservoir) pressure, and P_1 is the ambient pressure. The data on which this correlation is based[7] cover a variety of monatomic, diatomic, and triatomic gases, and the correlation was found to be independent of the specific heat ratio γ for $15 \leq P_0/P_1 \leq 17{,}000$ within the accuracy of the experimental data. Although the data used to derive the correlation were based on gases at low temperatures, the correlation also has been found to be valid for arc-heated free jets of highly ionized argon.[8] Recently, it has been shown[9] that the above equation

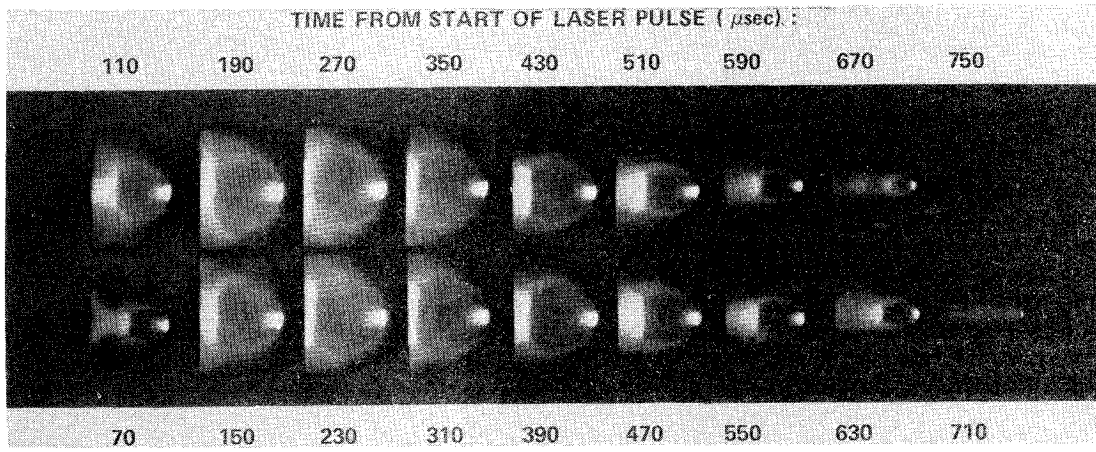

Fig. 6 High-speed photographs of free-jet development during pulsed-laser vaporization of graphite: pulse length = 800 μsec; exposure = 8μsec/frame; $q_{max} = 9.1 \times 10^5$ W/cm^2; $P_1 = 23$ Torr.

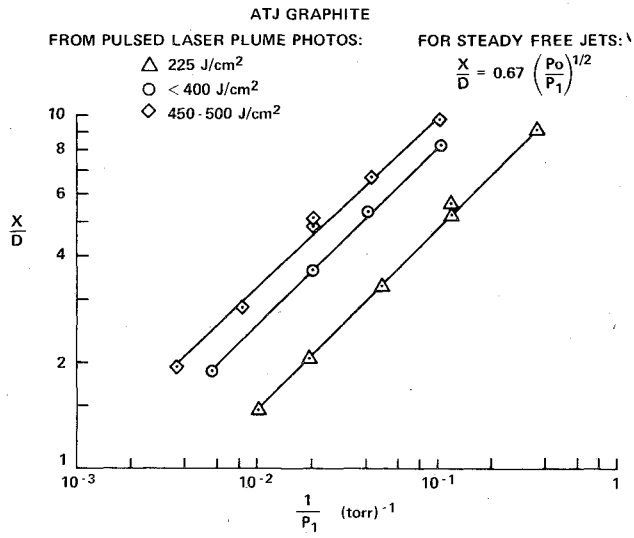

Fig. 7 Correlation of free-jet Mach disk displacement with ambient pressure and laser energy density.

is justified on theoretical grounds but with the proportionality coefficient weakly dependent on γ.

The validity of applying the correlation derived for steady free jets from orifice flows to transient free jets from planar surface vaporization was tested by experiments with graphite in which the ambient pressure was varied while the laser heating conditions were held constant. In using the aforementioned relationship, x was taken as the relative distance from the vaporizing surface to the center of the Mach disk image as recorded on time-integrated photographs, D was interpreted as the relative diameter of the surface area heated by the focused laser beam, and P_1 was again the ambient pressure. As discussed above, the Mach disk location measured on time-integrated pictures is that for the maximum displacement of the shock from the surface. This, in turn, corresponds to the peak surface temperature conditions. The peak surface temperature and surface pressure were invariant, since the laser pulse duration, peak energy flux, and total emission energy were constant. The data taken to test the applicability of the steady, free-jet correlation are presented in Fig. 7. The linear nature and the half-power slope of the results show that the relationship between the normalized Mach disk location and pressure given by Eq. (1) is also valid for free expansions from vaporizing surfaces.

Surface Condition Effects

The three materials considered cover a range of surface conditions from rough and porous for polycrystalline ATJ graphite to very smooth and dense for vitreous carbon, with pyrolytic graphite (surface normal to the c axis) having a roughness in between. At the vapor-solid interface, the mean free path of carbon vapor species range from the order of 10 μm at 3500 K to 0.1 μm at 4500 K if thermochemical equilibrium exists. It might be expected that details of the vaporization and initial vapor expansion may depend on whether the mean free path is greater or smaller than the dimensions of surface features, and scanning electron microscope (SEM) photomicrographs were made to characterize vaporized surface areas of the three carbons.

Figure 8 shows portions of vaporized ATJ and pyrolytic graphite surfaces magnified 2000 times, and it is seen that the microscopic scale of the ATJ surface is considerably larger than that of pyrolytic graphite. In contrast, Fig. 9 is a SEM photomicrograph of vitreous carbon at three magnifications. The top photograph shows a surface exposed once to a pulsed-laser beam. The vaporized area within the shallow crater gives a mapping of the radiation flux spatial distribution and shows the beam to be quite uniform and non-Gaussian. The center

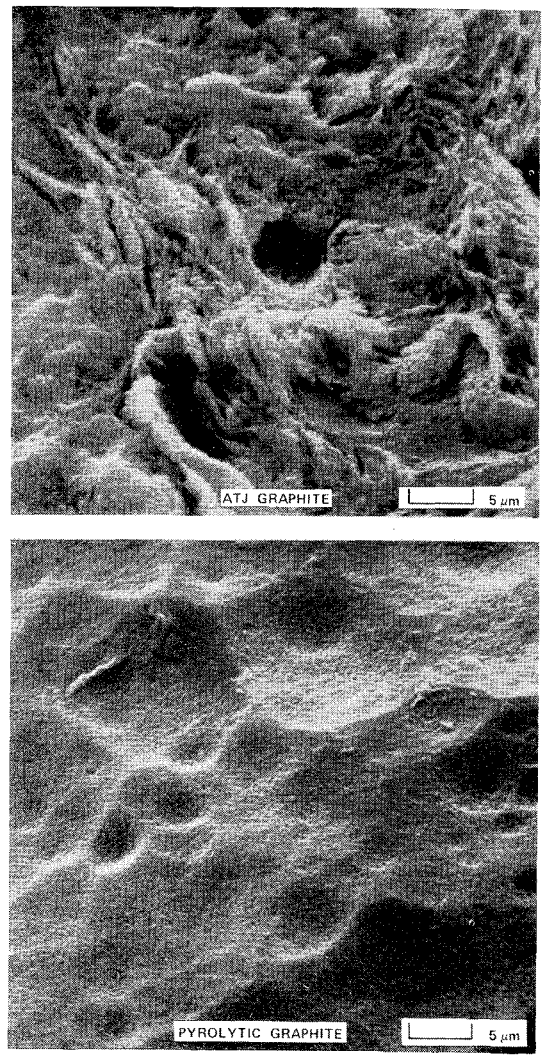

Fig. 8 SEM photomicrographs of vaporized ATJ and pyrolytic graphite surfaces (2000 × reduced 34%).

photograph shows a higher magnification of the central area of the top photograph, and indicates the very smooth nature of the vaporized surface and the limited extent of microcracking. The dimpled appearance reflects the variation of energy in the beam due to the mode structure of the electromagnetic field within the laser itself. The bottom view of Fig. 9 is a highly enlarged section of the crack area seen at left center in the middle photograph.

For the range of surface temperature (3600-4500 K) observed in this work, it is probable that the ratio of the vapor mean free path to a characteristic surface roughness length varied from less than to greater than unity at the ATJ graphite surface (Fig. 8), whereas this ratio was always greater than unity over the predominant, uncracked areas on the vitreous carbon surface (Fig. 9). Since observed free-jet flows from all three carbons were indistinguishable, it was concluded that, macroscopically, the vaporization and initial vapor expansion are independent of microscopic surface roughness.

Vaporization and Gasdynamic Considerations

A vaporization pressure can be derived, as was previously suggested, by applying Eq. (1) to the observed displacement of the free-jet Mach disk and, in analogy with free-jet flows from orifices, interpreting this pressure to be the same as the total pressure P_0 in the flow. Plotting this derived total pressure against the corresponding measured surface temperature results in the data for carbon vaporization given in Fig. 10. Here the experimental data are compared to

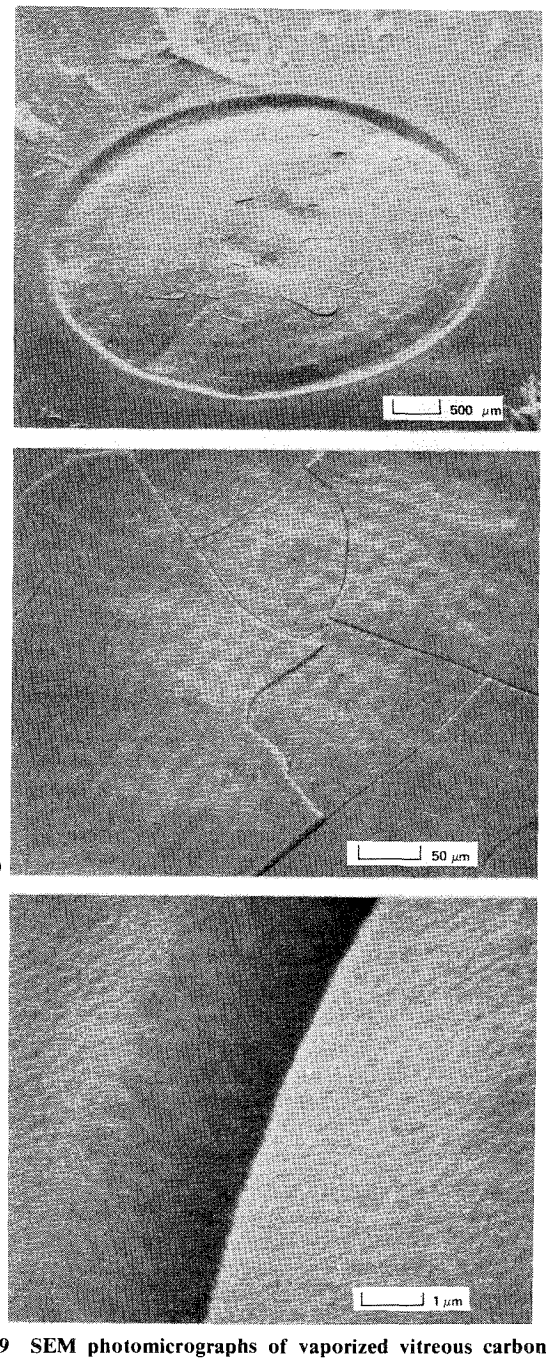

Fig. 9 SEM photomicrographs of vaporized vitreous carbon surfaces. a) 20×, b) 200×, c) 10,000×; all reduced 34%.

predictions of the vapor pressure of monatomic, diatomic, and triatomic carbon species as well as the total pressure of a system composed of these three species in thermochemical equilibrium with solid carbon. Mass spectrometric studies[10] of carbon vaporization have established that these particles are the major, and C_3 the predominate, species present in the saturated vapor phase at high temperatures. The JANAF curves are based on the thermodynamic data of Ref. 11. The good agreement in Fig. 10 between the data and extrapolated vapor pressure suggests that the gasdynamic total pressure is equal to the equilibrium vapor pressure.

Such an interpretation of the derived vaporization pressure must be made with caution, however, since there are several factors that can effect the comparison of experimental data and predicted vapor pressures. First, there is the problem of accurate surface temperature measurements at these high levels because of vapor absorption, surface emissivity, and instrument calibration uncertainties. Also, the vapor pressure

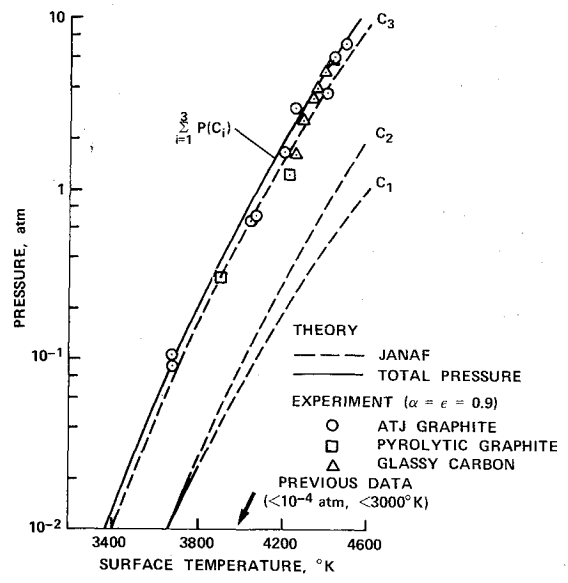

Fig. 10 Comparison of derived and extrapolated vapor pressures for carbon.

predictions are based on other data obtained at much lower pressures ($<10^{-4}$ atm) and temperatures (<3000 K), and the errors in extrapolation to these higher temperatures may be large so that a quantitative comparison with our data is not warranted. There is the related question not considered here of whether phase equilibrium exists at a phase boundary with a high mass flux and bulk velocity of vaporized species away from the surface. One study of this problem[12] indicates that the outgoing evaporation flux would be several times the recondensation flux to the surface, thus violating a condition classically assumed necessary for equilibrium vapor pressure measurement. However, a concurrent study,[13] using the Knudsen-Langmuir equation with experimental mass loss data from continuous wave laser vaporization of graphite, finds vaporization pressures that are in general agreement with the data shown in Fig. 10.

The similar nature of free jets from orifice and vaporization sources suggests that the vapor velocity should be sonic at or near the vaporizing surface by analogy with the sonic orifice. It can be shown that the velocity of a gas undergoing sudden expansion into vacuum is initially equal to the local acoustic velocity,[3] and models have been proposed[1,14] for vapor expansion from laser-heated surfaces that assume the velocity is sonic at the surface. However, the sonic point may not actually coincide with the vapor-solid interface since the velocity within several mean free paths of the surface depends on details of vaporization mechanisms and the gasdynamics of vapor expansion (including laser radiation absorption, if important) on a microscopic scale.[12] The location of the sonic condition cannot be determined from the photographic data given here but, in a macroscopic view, they do indicate that the vapor velocity can be considered sonic at a plane through the mean material surface. The vapor flow beyond this point clearly becomes a three-dimensional, supersonic expansion that can be analytically described by the same methods appropriate for axisymmetric, free-jet expansions downstream of a sonic orifice.[6]

Possible Applications

The good agreement between the derived pressure and the predicted for carbon equilibrium vapor pressure, as shown in Fig. 10, suggests that this may be a promising new technique for measuring the equilibrium vaporization pressures of refractory materials at high temperatures that are unobtainable by other means. Although the interpretation of this derived pressure as being equivalent to the vapor pressure of a system in phase equilibrium is still open to question,

preliminary data from carbon indicate a direct relationship between the two pressures. The major limitation appears to be the accurate measurement of surface temperature.

Another possible application of vaporization free jets is the formation of free-molecule beams of high-energy atomic and molecular species. The techniques for extracting a low-density, collisionless beam from the vaporization flow using skimmers and collimators are well established, and the use of laser vaporization sources offers the advantage of uncontaminated beams having energies and intensities higher than those obtainable from other sources. As an example, free-molecule flows of C_3 molecules with energies greater than 1.5 eV have been measured from the vaporization of graphite.[4]

Summary and Conclusions

It was shown that the vaporization of carbon and other refractory materials by burst-mode, pulsed-laser irradiation at power densities up to 2.5 MW/cm^2 can result in free-jet expansions of vapor products from planar surfaces. Time-integrated and time-resolved photography as well as mass flux distribution measurements have been used to establish the similarity between free jets from transient vaporization sources and those from sonic orifice flow sources. Surface photomicrographs were used to show that the vaporization and vapor expansion near the surface can be considered planar and independent of surface condition. The photographic data indicate that flows from laser-vaporized surfaces become sonic at or very near the surface by analogy with free jets from orifice flows. The location of the sonic condition cannot be defined from these photographs, but it is clear that the flow becomes three-dimensional and supersonic downstream of the sonic point.

Photographs of the Mach disk location within free-jet flows can be used to deduce the vaporization pressure during a laser pulse. This derived vaporization pressure, as a function of measured surface temperature, was found to be in close agreement with the equilibrium vapor pressure of carbon as predicted by the extrapolation of available data obtained at lower temperatures. Uncertainties in extrapolated carbon vapor pressures at these temperatures and pressures, and in the experimental measurements of Mach disk location and surface temperatures, leave open the question of the phase state at the vaporizing surface and the correct interpretation of the derived vaporization pressure. However, these results indicate that use of shock wave geometry in free jets generated during laser vaporization may be a promising new technique for determining vapor pressures of refractory materials at high temperatures.

References

[1] Krokhin, O. N., "Generation of High-Temeprature Vapors and Plasmas by Laser Radiation," *Laser Handbook*, Vol. 2, Elsevier, New York, 1972, pp. 1371-1407.

[2] Ready, J. F., *Effects of High-Power Laser Radiation*, Academic Press, New York, 1971.

[3] Zel'dovich, Ya. B. and Raizer, Yu. P., *Physics of Shock Waves and High Temperature Hydrodynamic Phenomena*, Vol. I, Academic Press, New York, 1966, pp. 101-106.

[4] Lincoln, K. A. and Covington, M. A., "Dynamic Sampling of Laser-Induced Vapor Plumes by Mass Spectrometry," *International Journal of Mass Spectrometry and Ion Physics*, Vol. 16, Jan. 1975, pp. 191-208.

[5] Batanov, V. A., Bunkin, F. V., Prokhorov, A. M., and Fedorov, V. B., "Immobile Shock Wave Produced Upon Stationary Evaporation of Metal by Laser Radiation," *JETP Letters*, Vol. 11, Jan. 1970, pp. 69-72.

[6] Ashkenas, H. and Sherman, F. S., "The Structure and Utilization of Supersonic Free Jets in Low Density Wind Tunnels," *Rarefied Gas Dynamics (Fourth Symposium)*, Vol. II, Academic Press, New York, 1966, pp. 84-105.

[7] Bier, K. and Schmidt, B., "Zur Form der Verdichtungsstösse in frei expandierenden Gasstrahlen," *Zeitschrift für angewandte Physik*, Vol. 13, Nov. 1961, pp. 493-500.

[8] Witte, A., Kubota, T., and Lees, L., "Experimental Investigation of a Highly-Ionized, Arc-Heated, Supersonic Freejet," *AIAA Journal*, Vol. 7, May 1969, pp. 870-878.

[9] Young, W. S., "Derivation of the Free-Jet Mach Disc Location Using the Entropy Balance Principle," *Physics of Fluids*, Vol. 18, Nov. 1975, pp. 1421-1425.

[10] Berkowitz, J. and Chupka, W. A., "Mass Spectrometric Study of Vapor Ejected From Graphite and Other Solids by Focused Laser Beams," *Journal of Chemical Physics*, Vol. 40, May 1964, pp. 2735-2736.

[11] Stull, D. R. and Prophet, H., *JANAF Thermochemical Tables*, 2nd ed., Vol. 37, June 1971, National Standards Reference Data Series, National Bureau of Standards (U.S.).

[12] Anisimov, S. I. and Rakhmatulina, A. K., "The Dynamics of the Expansion of a Vapor When Evaporated Into a Vacuum," *Soviet Physics JETP*, Vol. 37, Sept. 1973, pp. 441-444.

[13] Lundell, J. H. and Dickey, R. R., "The Vaporization of Graphite in the Temperature Range of 4000 to 4500 K," AIAA Paper 76-166, Washington, D.C., Jan. 1976.

[14] Pirri, A. N., "Analytic Solutions for Laser-Supported Combustion Wave Ignition Above Surfaces," *AIAA Journal*, Vol. 15, Jan. 1977, pp. 83-91.